Journal of Cleaner Production 80 (2014) 170–178

Contents lists available at ScienceDirect

Journal of Cleaner Production

journal homepage: www.elsevier.com/locate/jclepro

Remanufacturing of turbine blades by laser direct deposition with its energy and environmental impact analysis

J. Michael Wilson, Cecil Piya, Yung C. Shin*, Fu Zhao, Karthik Ramani

School of Mechanical Engineering, Purdue University, 585 Purdue Mall, West Lafayette, IN 47907, USA

ARTICLE INFO

Article history:
Received 30 October 2013
Received in revised form
26 May 2014
Accepted 27 May 2014
Available online 5 June 2014

Keywords:
Remanufacturing
Laser direct deposition
Life cycle analysis
Turbine blade repair

ABSTRACT

Laser direct deposition provides an attractive and cost effective means for repairing or remanufacturing high value engineering components. This study demonstrates the successful repair of defective voids in turbine airfoils based on a new semi-automated geometric reconstruction algorithm and a laser direct deposition process. A Boolean difference between the original defective model and the final reconstructed model yields a parameterized geometric representation of the repair volume. The experimental results of this method demonstrate the effectiveness of laser direct deposition in remanufacturing and its potential to adapt to a wide range of part defects. A Life Cycle Assessment (LCA) on the energy and environmental impacts by remanufacturing is also presented.

1. Introduction

Sutherland et al. (2003) presented that rising concerns over escalating emissions, resource depletion, and other environmental issues have led to an increased emphasis on the design and manufacturing of environmentally benign products. Consequently, Ramani et al. (2010) describes that remanufacturing has emerged as a promising practice to reduce the environmental impact of products by extending their lifespan and thus precluding the need for consistent replacements that are costly in terms of both energy consumption and financial expenditure. Its value can be understood by analyzing the results of a recent study conducted by the Department of Defense, which evaluated used components worth over $100M in the Corpus Christi Army Depot to be amenable to repair and a new life through laser-based remanufacturing according to Hedges and Calder (2006).

Aerospace and automotive components are susceptible to wear and damage over time. Many of these components reach their "end of life" stage prematurely due to limitations prevalent in overhauling techniques. This problem arises due to the fact that most of such components use high strength alloys, which help achieve good thermo-mechanical properties but also present challenges in manufacturing. Such materials require special tooling and consume a significant amount of energy during manufacturing processes. This cost is further exacerbated by the high financial expenditure associated with purchasing the necessary raw materials and conducting requisite manufacturing processes. Consequently, a cost effective and efficient repair process is necessary to remanufacture such damaged components.

Teams of researchers, Grant and Tabakoff (1975) and Antony and Goward (1988), indicated that damage in high valued metallic components is often found in the form of cavities or voids in the material. As the material degrades or the critical dimensions of the component no longer match the specified dimensions required for efficiency, the performance of the component also diminishes. After remanufacturing, these components can regain all of their efficiency, or regain even more, by incorporating more advanced materials or by adapting to the improved design.

In the past there have not been any good methods to remanufacture these kinds of voids or cracked parts in a cost effective manner as described by Zhang et al. (2002) and Bonacorso et al. (2006). Traditionally welding has been the primary method used to restore shape and functionality of damaged aerospace and automotive components. The welding process is often very manual and tedious. Gas Tungsten arc welding (GTAW) is one example of the welding repair processes. Eiamsa-ard et al. (2005) showed that the bonding between the filler material and the damaged part provided by GTAW is poor and unreliable for high performance mechanical parts. Other problems related to GTAW are its incompatibility with a wide range of advanced materials and the high operating temperatures (up to 5500 °C) that can be detrimental to the parts being repaired. Furthermore, manual welding repair

* Corresponding author. Tel.: +1 765 494 9775; fax: +1 765 494 0539.
E-mail address: shin@purdue.edu (Y.C. Shin).

http://dx.doi.org/10.1016/j.jclepro.2014.05.084
0959-6526/

typically requires manual grinding after the welding is completed, causing the process to become even slower, less automated, and consequently less accurate. Recently, Roy and Francoeur (2002) introduced the refined process using micro arcs to weld filler material onto the substrate. However, Francoeur (2002) indicates that this method is still contingent upon the skill of the welder, and falls short of an efficient automated process.

Smith and Keoleian (2004) and Östlin et al. (2009) showed that the advent of accurate material additive processes has made such repair not only economically viable, allowing the restoration of the shape back to its correct dimensions, but also facilitates design enhancements at the time of remanufacturing. By utilizing the knowledge attained from observing the product's past performance, its weakness can be strengthened and design improvements can be incorporated into its current framework. Furthermore, Michaud and Llerena (2006) presented that remanufacturing also cuts down the cost for waste disposal, since it builds upon the non-damaged portion, which is close to its final form, and thus requires only a fraction of material processing. Consequently, remanufacturing by accurate additive processes will enable industries to save energy and material, and contribute towards sustainable design and manufacturing.

The advancements made in additive manufacturing technologies have provided a strong prospect for the automation of the aforementioned repair process with a significant increase in the accuracy of the final repair. One of such promising material additive processes is laser direct deposition (LDD) or laser engineered net shaping (LENS®). LDD has been commonly used in rapid prototyping of fully dense parts by Dutta et al. (2011). Such deposition systems are combined with computer numeric control (CNC) and computer aided design (CAD) systems that provide a flexibility, which lends itself to many different remanufacturing applications.

Since a part begins to wear after a number of cycles of operation, the original CAD model may not reflect the geometry of the worn part. In addition there are occasions when the Original Equipment Manufacturers (OEM) does not choose to remanufacture their own products as described by Gutowski et al. (2011). In these scenarios third-party remanufacturing firms are left to break down and reverse engineer the products without the aid of the original CAD model. When an accurate 3-dimensional (3D) model is not available, a reverse engineering process is required in order to reconstruct a geometric representation. Here, a 3D digitized mesh of the defective part and a surface reconstruction algorithm are applied to define part geometry. Moreover, the surfaces reconstructed are closely associated with a parametric representation, which enables manipulation of the surface geometry. Consequently, the geometric models of the defective part are amenable to a "virtual repair" process, which further enhances the quality of the actual repair.

Presently, LDD remanufacturing methods for high value metal components are inadequate. There has been a lot of focus on seamlessly moving from the digital data to a tool path used by the laser direct deposition machine, but few have discussed ways to increase the performance of the product while still accurately reconstructing the missing geometry. Gao et al. (2008) and Yilmaz et al. (2005) have focused on automating the repair of a specific type of component such as turbine blades. Bremer (2005) and Gao et al. (2010) addressed a more general repair solution for any geometry type. Yilmaz et al. (2010) automated the process of digitizing and meshing, and reconstructed the geometry from a digitized polygonal model using non-uniform rational b-splines (NURBS).

In this study laser direct deposition is employed to restore a damaged turbine blade. A previously developed algorithm by Piya et al. (2011) is used to reconstruct a model of a defective region of the turbine blade airfoil. This algorithm uses the Sectional Gauss Map concept to extract Prominent Cross Sections (PCS) from a mesh object. The PCS extracted from a defective airfoil mesh is thus utilized to facilitate semi-automated reverse engineering and geometric reconstruction of a component with complex geometry. The accuracy of these results is compared to a reference model generated entirely in a CAD system. Strength tests were carried out to validate the strength of the repair. Finally, a Life Cycle Assessment (LCA) is performed on the LDD process, and the environmental impact results are compared between the LDD-based remanufacturing of a turbine blade and complete blade replacement.

2. Prominent Cross Section (PCS)

To facilitate accurate tool path generation for the LDD process, a geometric model of the repair volume must be available. This section describes the algorithmic theory behind the PCS and its use in extracting a parameterized CAD model of the repair volume.

Sellamani et al. (2010) introduced a PCS at a point on the surface of a solid object, which is defined as the cross-section of the local sweep segment passing through that point. Fig. 1 illustrates two PCS (C1 and C2) corresponding to two seed points (P1 and P2) in a hyperboloid CAD model. Here, both PCS are part of the same sweep segment and lie normal to the sweep direction. A PCS at a point is obtained through a series of iterative steps, each entailing the following steps:

1. Slicing the CAD model by a cutting plane that passes through the given seed point. The orientation of the cutting plane in the first iteration lies along the maximum curvature direction and the surface normal at the seed point.
2. Extracting normal vectors of all mesh facets that intersect with the cutting plane.
3. Generating a Sectional Gauss Map by plotting the normal vectors into a unit sphere. The points of intersection between these vectors and the unit sphere are referred to as the Sectional Gauss Map data.
4. Obtaining a new and refined cutting plane orientation through the least squares method applied on the Sectional Gauss Map data. This orientation will be applied to the cutting plane of the ensuing iteration.

This iterative process is repeated until the angular difference between cutting planes of two consecutive iterations (error value) falls below a user-defined threshold. The curve of intersection between the final cutting plane and the CAD model yields the PCS at that particular seed point. Furthermore, to enhance the robustness of the method, the same iterative process is carried out at the given

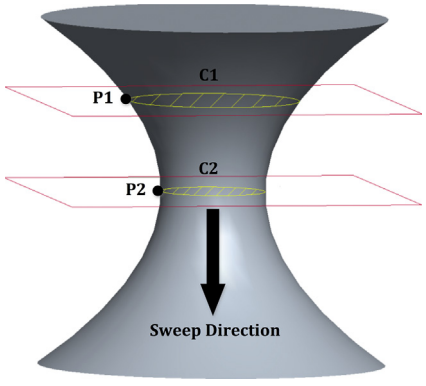

Fig. 1. Prominent Cross Sections on a hyperboloid.

seed point with a cutting plane aligned along the minimum curvature direction and the surface normal. Consequently, for each seed point we end up with two PCS. Empirical results have indicated that the final cutting plane with a lower error value provides a more accurate PCS amongst the two. Fig. 2 illustrates the iterative process involved in PCS generation at a given seed point P.

Fig. 3 illustrates the extraction of PCS from the non-defective region of an airfoil that has a chunk missing from its body. The following sections will describe the use of the PCS to reconstruct a virtually repaired model from which the geometric representation of the repair volume can be extracted. For detailed information on this process, refer to Piya et al. (2011).

3. Experimental procedures

This section is broken into 2 parts; the first part shows the geometry reconstruction process and the second part shows the procedure for tensile testing of an aerospace superalloy. For the reconstruction portion, the focus was on the geometry and not the material.

3.1. Reference model construction

A turbine blade was selected as the part to be restored to demonstrate the proposed geometric reconstruction methodology. A repair scenario was set up by constructing a SS316L turbine blade with a missing section in the tip area by means of laser direct deposition as shown in Fig. 4. Hamed et al. (2006) indicate that turbine blade damage commonly occurs in the tip portion of the blade. This damage can affect the performance of the entire engine. Because of defects and distortions, each blade is unique. It is critical that the damaged area be accurately reconstructed or safety and performance may be compromised.

Typically, the damaged blade is scanned and digitized into a point cloud, which is then transformed into a meshed representation comprising triangular facets that collectively provide the net shape of the blade. For this study, a mesh of an existing turbine blade with a user induced experimental defect was used to construct the repair volume. As a result the point cloud acquisition step in Fig. 5a is hypothetical in the current study but nonetheless represents real world practices. The PCS algorithm was run on the mesh surface of the defective blade model and the resulting PCS data, lying strictly over the non-defective region of the blade, was imported into CATIA™ V5 by means of a custom Microsoft® Visual Basic macro. In CATIA™, the PCS points in the non-defective region are read and utilized for the construction of splines that represent incremental blade cross sections of the non-defective region as shown in Fig. 5b. Each spline is smoothened with a tangency specification of 0.5°. Following this, a surface is swept across the spline cross sections and then the surface is extrapolated over the remaining height of the blade, spanning across its defective region. A solid body is thus built from the resulting combination of surfaces (PCS + extrapolated), as shown in Fig. 5c. Once the extrapolated surface is created, a Boolean operation is performed to extract the difference between the reconstructed ("virtually" repaired) blade and the original meshed surface of the defective blade model, leaving us with the desired repair volume as seen in Fig. 5d.

3.2. Blade restoration

The experiments were carried out on an Optomec LENS® 750, equipped with an IPG fiber laser (CW, TEM00), which has a maximum power capacity of 500 W and a maximum work envelope of 300 × 300 × 300 mm. Experiments were run with a laser spot size of 600 μm with an approximate distance of 9.5 mm between the bottom of the powder spray nozzles and the top of the part target surface. Stainless Steel 316L powder with the average size of 44 μm was used as the material in the experiment to show the geometry reconstruction method and due to its low cost and availability. The system is equipped with an argon environment to prevent any oxidation and chemical reactions during deposition. Each layer consisted of a contour deposition step and hatch deposition step. At the end of each layer the Z height was adjusted automatically according to the layer spacing parameter and the hatch angle was rotated. The hatch angle was set to 0, 45, 90 and 135°, returning to the original hatch orientation after every 5 layers. A schematic illustrating the laser direct deposition is shown in Fig. 6 and all the operating parameters are listed in Table 1.

With the "virtually" repaired model, a tool path was generated for each repair. From the tool paths, two 61 mm blades were built using the LDD process. The blades were built with a defective region and were used for experimental repair. The first blade was repaired using repair geometry that was extracted from a nominal reference (non-defective) model by separating the required repair area from its main body with a set of planar surfaces as shown in Fig. 7. Such repair is only valid in cases where a nominal model is available. The second blade was repaired using repair geometry produced from the PCS method described in the previous section. This repair provides its value in cases where a nominal model is not present, and the repair needs to be based on the geometry of the existing non-defective region.

3.3. Tensile testing

Two cylindrical tensile samples were built with laser direct deposition to determine the strength of LDD repaired parts. A

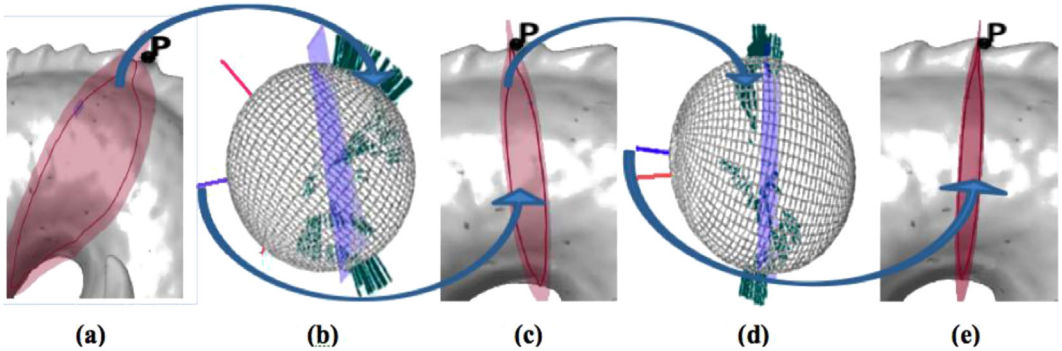

Fig. 2. Optimizing a cutting plane at point P with Sectional Gauss: (a) initial cross section along normal and maximum curvature directions at point P, (b) initial Sectional Gauss Map, (c) cross section after few iterations, (d) Sectional Gauss Map at that iteration, (e) final PCS.

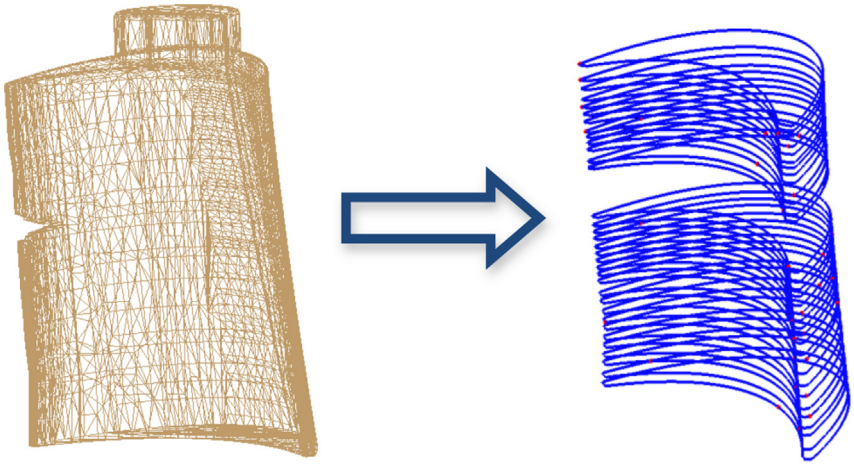

Fig. 3. Extracting PCS from the non-defective regions of an airfoil.

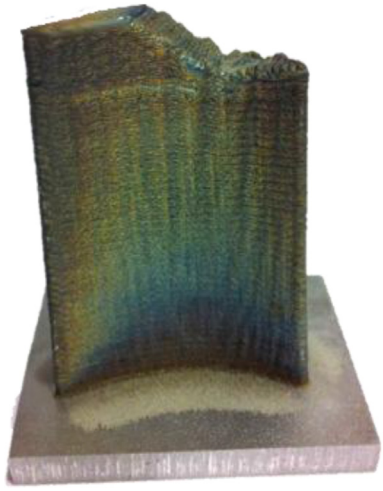

Fig. 4. Damaged turbine blade built with laser direct deposition.

nickel-based superalloy (Nistelle 625 from Deloro Stellite®) with a powder size of 90 μm/45 μm was used, which has a weight % composition of Ni-bal Fe-5 C-0.1 Cr-21.5 Mn-0.5 and Mo-9. This material was selected based on its high performing properties and extensive use in aerospace applications. Dimensions of the specimen were made according to the ASTM E8 standard for round samples with an extended reduced cross section to accommodate a 2-inch extensometer. Laser power was set to 300 W with the scanning speed at 13.12 mm/s. Powder flow was 12.5 g/min and hatch/layer spacing was 0.46 and 0.30 mm respectively. The first specimen was built the full height (128.5 mm) and the second specimen was initially built to approximately half the total height (65 mm). One hour was allotted to allow for complete cooling and then the top surface of the second specimen was ground with a hand file until the surface was flat and shiny. Finally, the remaining portion of the build was completed.

Final machining was done on a Haas SL10 CNC lathe to obtain the final shape and the location of the repair was maintained in the center of the specimen. Tensile testing was performed on a Sintech 30/D MTS machine. The machine possessed a load capacity of 100 kN (22,000 lbf). The grips were wedge shaped and the clamping force was adjusted manually. A strain rate of 1 mm/min was used to fracture the two samples.

4. Results and discussion

4.1. PCS accuracy

A distance analysis tool inside of CATIA™ V5 Free Form workbench was utilized for demonstrating the accuracy of the reconstruction. In this analysis, the PCS repair geometry was aligned with the appropriate corresponding region of the reference model. A statistical distribution was calculated to determine the locations in

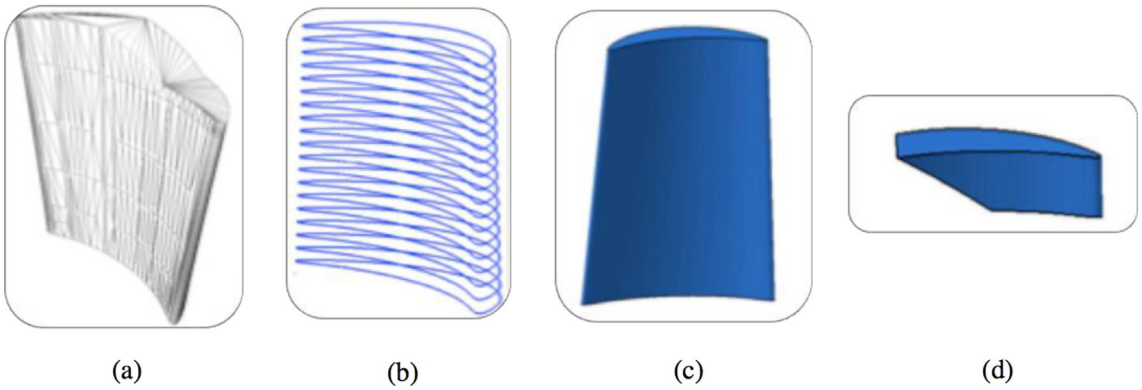

Fig. 5. Process for generating a parameterized geometric model required for LDD based defect repair: (a) acquire point clouds and generate mesh, (b) extract PCS from non-defective region and extrapolate missing section, (c) reconstruct repaired model in CATIA™, and (d) extract Boolean difference between (a) and (c) to obtain the repair volume.

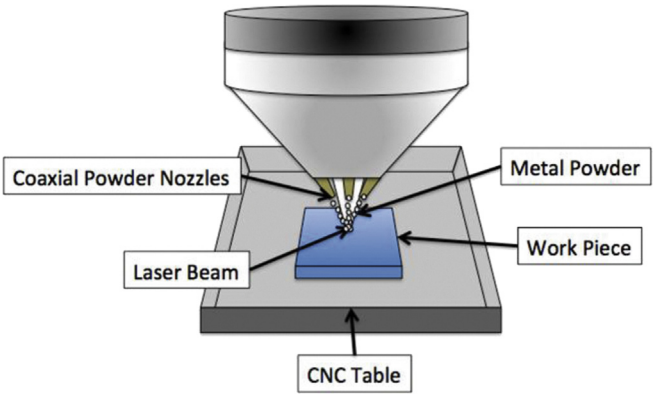

Fig. 6. A schematic of the laser direct deposition.

Table 1
Parameters used in the LDD repair process.

Parameters	Nominal repair volume	PCS repair volume
Number of Layers	18	18
Scanning speed (mm/s)	11.4	12.3
Hatch spacing (mm)	0.533	0.457
Layer Spacing (mm)	0.356	0.356
Powder flow rate (g/min)	22.1	18.5
Laser power (W)	375	375
Total cycle time (min)	14	18

the repair geometry with the greatest deviation. The maximum deviation from the nominal model was 0.145 mm with most of the deviation less than 0.030 mm, which is within the aerodynamic profile tolerance (0.050 mm) of a turbine blade according to Bunker (2009). Since the strength of the PCS algorithm depends on the appropriate distribution of mesh density across the model: regions with a rapid change in shape require more facets for accurate representation. For example, the trailing edge has a high degree of curvature, thus accuracy on the trailing edge is less than that of the concave side of the blade with less curvature. Greater accuracy can be achieved by exporting a finer mesh from the CAD system.

Due to the fact that the PCS repair geometry was derived from splines some additional error may have been introduced.

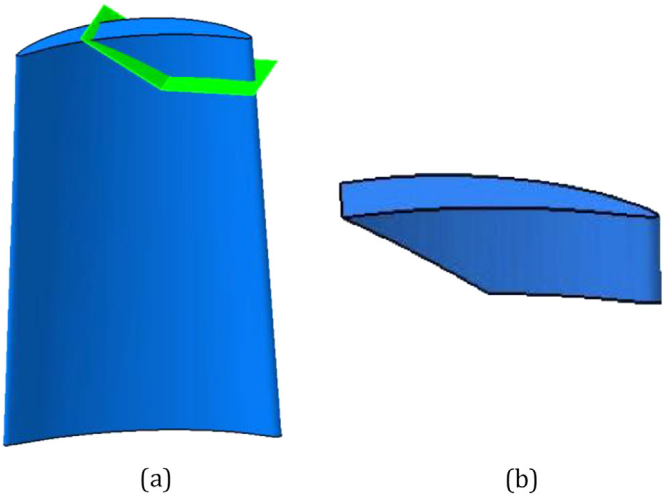

Fig. 7. Process for generating a repair volume required for laser direct deposition: (a) construct damaged region with extruded surface, and (b) extract repair volume by splitting the airfoil body with the extruded surface.

Mohaghegh et al. (2010) indicates that the geometry of the airfoil is usually reconstructed with arcs rather than splines. Splines can have many degrees of freedom and make optimization more complicated. There is a combined effect from having excessive control points in the spline and excessive PCS that caused the repair section to have fluctuations.

4.2. Laser direct deposition build

Fig. 8 shows the results of the two LDD repairs compared to the nominal case. The total build time for the nominal and PCS repair was 14 min and 18 min respectively. The total repair volume was 770.2 mm^3 and had a mass of 5.9 g, which comprised 5.1% of the total volume. Due to the nature of the geometry, with each z increment, layers required more tracks and time to fill the missing area. The area of the first layer was 70.25 mm^2 increasing to 162.62 mm^2 on the 18th layer. As shown in Fig. 9 the total height of the repair is somewhat greater than the height of the non-repaired portion. Height differences occur due to tolerance capabilities in the LENS® system. A slight overbuild was necessary to account for these differences and excess material is later machined as a post LDD process. The final geometric tolerance was within 150 μm, while the majority of the restored part was within 30 μm of the desired geometry. This demonstrates that the LDD process can restore the shape to the near net-shape, requiring virtually little secondary machining.

4.3. Registration and alignment

Even though consistent coordinate systems were maintained throughout the process, a different origin point must be defined in the LDD tool path software. The tool path software automatically calculates the geometric bounding box of the input geometric model. Regardless of where the geometry resides in the CAD system the start point is determined to be 2.54 mm from the minimum *X* and minimum *Y* coordinates.

Fig. 10 demonstrates how the origin point is determined by showing the 2 layers with the minimum coordinate values in the *x* direction (Layer 240) and the *y* direction (Layer 1). Because the blade twists, the minimum *x* is found on the top of the blade and minimum *y* is found on the first layer of the blade. Consequently, a new repair model with the same overall dimensions as the undamaged model was constructed. This was done by building a bounding box around the reconstructed turbine blade model and extruding a solid up to the bottom of the repair surface as shown in Fig. 10.

4.4. Tensile testing

The as-deposited properties of the tensile samples at room temperature were within the range found from experimental data of other laser additive builds of Nistelle 625 (Inconel 625) as seen in Table 2. Both the repair sample and the undamaged sample had an ultimate strength and yield strength that was consistent with annealed bar.

Both samples broke near the upper grip away from the central repaired region. Repair performed by LDD was just as strong as the original material. These tests furthered strengthened the use of LDD for remanufacturing.

4.5. Environmental impacts of remanufacturing by LDD

As with other manufacturing processes, a considerable portion of the environmental impacts stems from the amount of energy required by the manufacturing process according the EPA (2009)

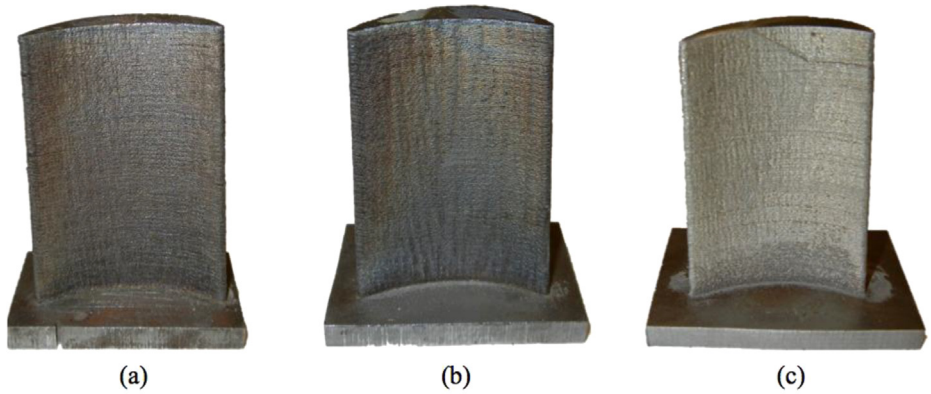

Fig. 8. Turbine blades built with the LDD Process. a) baseline undamaged blade, b) nominal restored blade and c) PCS restored blade.

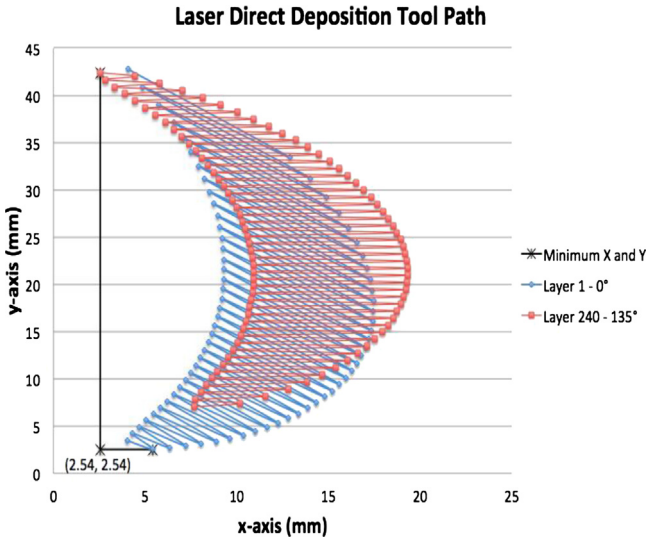

Fig. 9. Laser direct deposition tool path of the undamaged blade.

and Franco et al. (2010). In order to quantify this impact, a Life Cycle Assessment (LCA) was performed. LCA considers the environmental impacts of a product or a process over its lifetime (cradle-to-grave) or over multiple lifetimes (cradle-to-cradle). A comparative LCA was conducted between the environmental impacts of re-manufacturing a damaged blade by the LDD process and creating a new blade by means of investment casting. Key assumptions for the study are that the lifetime and performance of the repaired blade are the same as a new blade. The scope of the LCA includes the inputs and outputs of the LDD and investment casting processes assumed to be most significant in regards to environmental impact. For LDD, the steps of cleaning the work part, digitizing the repair area, reconstructing the CAD model, and qualification were not included in the study due to the relatively small impact these steps have in comparison to the actual metal deposition phase.

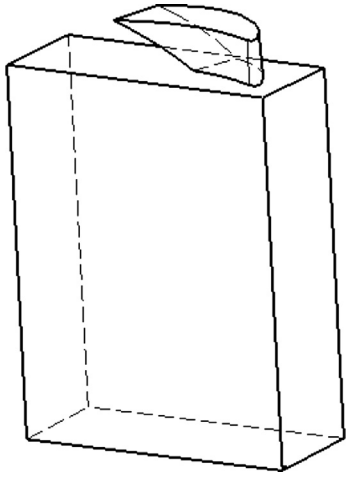

Fig. 10. Turbine blade bounding box for repair build.

Fig. 11 shows the system boundaries for both portions of the study. The system boundaries of the laser direct deposition process do not consider the pre-processing step including cleaning and pre-machining the repair surface. The inputs to the system are the damaged blade, metal powder, argon and electricity. The system boundaries for the investment casting process include all of the energy used to form the patterns and mold, melt out the pattern, and fire the mold. In addition, the energy to process the raw metal used in the casting process is included. The use of wax, plastic, binders, and refractory slurry and grain is excluded due to the relatively small impact of these materials on the carbon footprint of the process.

For this particular study the functional unit, a unit used as a reference for the environmental impacts of the process, is defined as one operational turbine blade made of a nickel alloy. This corresponds with the amount of material used in the theoretical application of LDD to repair a 95.6 cm^3 section on a 30.5 cm (12 inch) turbine blade compared with fabricating a new blade of equal size. The mass of the blade and the mass of the repair presented in this study are 15.6 kg and 0.78 kg respectively.

Table 2
LENS Inconel® 625 vs. Annealed Inconel 625.

Process	Ultimate tensile strength (MPa)	Yield strength (MPa)	Elongation (%)	Reference
Annealed bar	841	403	30	Griffith (2000)
LENS	938	584	38	LENS (2011)
LENS	931	614	38	Griffith (2000)
Laser consolidation	744	477	48	Xue and Islam (2002)
Laser rapid manufacturing (LRM)	920	572	48	Paul et al. (2007)
LRM	690	540	36	Ganesh et al. (2010)
SLS + HIP	855	490	N/A	Santos et al. (2006)
LENS repair	793	482	56	–
LENS undamaged	815	487	69	–

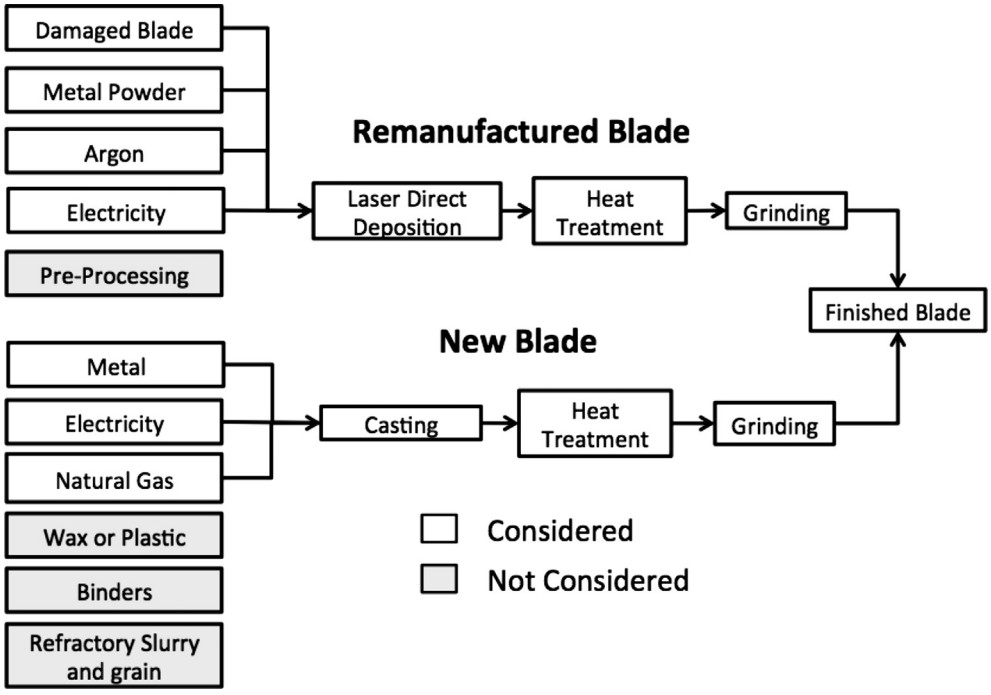

Fig. 11. System boundaries for the both processes.

Table 3
Operating parameters and material/energy flows within the scope of the study for laser direct deposition for a 5% blade volume repair.

Life cycle inventory (LCI)	Amount	kg CO_2 eq	Energy (MJ)	Source	Eco-invent entry
Metal in bar stock form	1.09 kg	22.7	304.8	Calculated	NiCr20Co18Ti I
Powder production	1.09 kg	3.6	60.6	Margolis et al. (1999)	–
Argon	16.67 kg	4.6	98.0	Calculated	Argon, crude, liquid, at plant
500 W-laser direct deposition system	17.8 h	70.1	1146.3	Manufacturer	–
Cleaning/finishing	0.78 kg	0.05	0.8	Margolis et al. (1999)	–
Total		101.0	1610.6		

The lifecycle inventory (LCI) was completed using Simapro 7.1, the Ecoinvent 2.0 database, and published government reports. For the LDD process, the amounts of argon and metal powder consumed were calculated using material consumption models derived from deposition builds previously mentioned in this paper. The energy consumed was calculated based on average usage data from the manufacturer. The system uses an IPG Photonics fiber laser with a wall plug efficiency of over 25% and a PC41 chiller rated at 3.6 kW. All auxiliary components of the laser system were considered including; the controls system, vacuum pump, and powder feeder motor. Because cycle time and actual repair energy usage vary based on laser input parameters, energy calculations for the LDD process considered a range of operating conditions. It was assumed that 40% of the powder was wasted and could not be recovered and that argon was consumed at 560.7 L/h. The energy requirements to remelt and atomize the metal were calculated using data shown by Morrow et al. (2007). The entry for NiCr20-Co18Ti was used as it closely represented the composition of super alloys used to make modern turbine blades. Heat treatment for this material requires a two-stage treatment, the first stage is held for 8 h at 1079 °C and then 16 h at 699 °C. Energy required for heat treatment was calculated based on the energy necessary to heat treat 1 kg of steel for 1 h, and finishing (blasting, chipping and grinding) operation was calculated based on Margolis et al. (1999). The finishing stage takes into account the cutting or trimming of flashing, gates or risers after the casting process is complete. A list of values used for the LCI for the LDD process is shown in Table 3.

The data used for the LCI of the investment casting was taken from a 1999 report published by the United States Department of Energy on the metalworking industry by Margolis et al. (1999). This

Table 4
Operating parameters and material/energy flows within the scope of the study for investment casting.

Life cycle inventory (LCI)	Amount	kg CO_2 eq	Energy (MJ)	Source	Eco-invent entry
Metal in bar stock form	16.4 kg	341.8	4586.7	Calculated	NiCr20Co18Ti I
Investment Casting	16.4 kg	16.9	286.7	Morrow et al. (2007)	–
Heat treatment	15.6 kg	7.6	133.2	Calculated	Heat treatment, hot impact extrusion, steel
Cleaning/finishing	15.6 kg	1.0	16.5	Margolis et al. (1999)	–
Recycling of damaged blade (credit)	15.6 kg	−0.7	13.8	Calculated	Iron scrap, at plant
Total		366.5	5036.9		

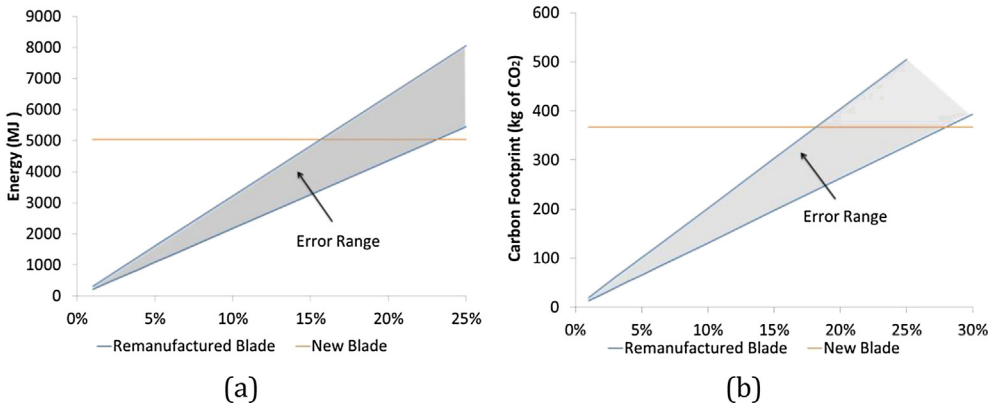

Fig. 12. (a) The total energy use and (b) potential environmental impacts of the LDD process in comparison with the investment casting process at different repair percentages.

Table 5
Operating parameters and material/energy flows within the scope of the study for gas tungsten arc welding (GTAW) for a 5% blade volume repair.

Life cycle inventory (LCI)	Amount	kg CO_2 eq	Energy (MJ)	Source	Eco-invent entry
Filler metal	0.975 kg	20.32	267.55	Calculated	NiCr20Co18Ti I
Argon gas	14.43 kg	2.72	63.96	Calculated	Argon ETH U
Electricity consumption for GTAW system	14.27 kWh	11.92	198.55	Calculated	Electricity, low voltage, at grid/US U
5-axis CNC grinding machine	99.09 kWh	82.78	1378.15	Calculated	Electricity, low voltage, at grid/US U
Cleaning/finishing	0.78 kg	0.05	0.8	Margolis et al. (1999)	–
Total		117.80	1908.95		

Table 6
Operating parameters and material/energy flows within the scope of the study for plasma transferred arc welding (PTA) for a 5% blade volume repair.

Life cycle inventory (LCI)	Amount	kg CO_2 eq	Energy (MJ)	Source	Eco-invent entry
Powder	0.975 kg	20.32	267.55	Calculated	NiCr20Co18Ti I
Powder production	0.975 kg	3.22	54.21	Margolis et al. (1999)	–
Argon gas	2.91 kg	0.55	12.90	Calculated	Argon ETH U
Electricity consumption for PTA system	6.95 kWh	5.81	96.70	Calculated	Electricity, low voltage, at grid/US U
5-axis CNC machine	99.09 kWh	82.78	1378.15	Calculated	Electricity, low voltage, at grid/US U
Cleaning/finishing	0.78 kg	0.05	0.8	Margolis et al. (1999)	–
Total		112.73	1810.30		

detailed report gives the energy requirements in the form of electricity and natural gas to produce a good casting. It should be noted that this report takes data applicable for the investment-casting sector as a whole, and does not specify the differences in energy and material flows for different metals. It was assumed that the damaged blade was recycled and used as scrap iron. It was assumed that after laser direct deposition only the repaired portion of the blade was cleaned and finished. Table 4 lists the entries for the LCI of the investment casting process in this study.

4.6. LCA impact assessment/interpretation

The impacts of the process were measured using the IPCC 2007 GWP 100a V1.01 and Cumulative Energy Demand V1.05 method. The IPCC method is a single-issue method that calculates the impacts from CO_2. The cumulative energy demand calculates the total demand from primary energy sources resulting from the production, use and disposal of an economic good (product or service) as suggested by Frischknecht et al. (2007). The total energy use and potential environmental impacts of the process are presented in Fig. 12. Upper and lower bounds were generated based on the laser power ranging from 250 W to 500 W.

An analysis of the impact assessment phase shows that the energy consumption and carbon footprint of using LDD to remanufacture a turbine blade can be significantly less than manufacturing a new blade. The quantity of kg of CO_2 saved is dependent on the amount of material to be repaired. Laser processing is energy intensive and most of the carbon footprint results from the electricity consumption of the laser deposition process. The total energy required for the LDD process was favorable in cases when less than 18% of the total blade volume needs to be repaired. Laser efficiency is continuously improving, thus providing potential for more efficient repairs and cost savings on repair. In the case of investment casting most of the impact was a result of extracting and forming the raw metal ingot. Because the repaired blade is already in its final form the amount of new material is drastically reduced and the CO_2 release resulting from early lifecycle stages is avoided.

There are some other methods such as gas tungsten arc welding (GTAW) and plasma transferred arc (PTA) welding that have been used for blade repair. Operating parameters and LCI entries for the GTAW and PTA process are shown in Table 3. It should be noted that in the PTA process the filler alloy is in powder form, so carbon emission and energy consumption due to powder production need to be considered.

Comparing Table 3, Table 5 and Table 6, it seems that GTAW and PTA processes release slightly more greenhouse gases and consume more energy, when considering the grinding process needed to remove material to generate the requisite shape. However, welding of high strength Ni-base super-alloys suffers from some fatal

limitations, such as thermal stresses due to huge heat input to the base materials and severe cracking (solidification cracking, grain boundary liquation cracking, and strain age cracking) in the welded layers (Bi and Gasser, 2011; Pinkerton et al., 2008). Therefore, blades repaired via GTAW or PTA do not have the same mechanical strength as new blades or blades repaired via LDD and may have quite limited usable life. From LCA standpoint, this suggests that GTAW or PTA based repair does not offer same "function", thus using the same functional unit for the three repair technologies cannot be justified. It is important to note the major assumption of this study is performance and lifetime equality between the two processes. Even a slight change in turbine efficiency could potentially change the magnitude of the carbon footprint of the processes in very significant ways. Impact categories such as ecotoxicity and carcinogens were calculated, but not presented due to the uncertainty of the data gathered.

5. Conclusions

LDD remanufacturing lends itself to repair "non-repairable" components in an environmentally friendly manner. This method demonstrated the effectiveness of laser direct deposition in remanufacturing and its ability to adapt to a wide range of part defects. This study succeeded in repairing defective voids in two turbine airfoils based on a new semi-automated geometric algorithm using a LDD system. The repaired blade matched the geometry of the original blade with mean accuracy of 0.030 mm. Mechanical testing was performed and found that a LDD repaired sample has good ductility and comparable strength compared to other forms of Nistelle 625 superalloy. A Life Cycle Assessment (LCA) on the energy and environmental impacts showed that LDD is most beneficial with relatively small defects. When the repair volume is 10% (1.56 kg) there is at least a 45% carbon footprint improvement and a 36% savings in total energy over replacing with a new blade.

References

Antony, K.C., Goward, G.W., 1988. Aircraft Gas Turbine Blade and Vane Repair. In: Reichman, S., Duhl, D.N., Maler, G., Antolovich, S., Lund, C. (Eds.), Superalloys. The Metallurgical Society., Warrendale, PA, pp. 745–754.

Bi, G., Gasser, A., 2011. Restoration of nickel-base turbine blade knife-edges with controlled laser aided additive manufacturing. Phys. Procedia 12 (1), 402–409.

Bonacorso, N., Goncalves, A., Dutra, J., 2006. Automation of the processes of surface measurement and of deposition by welding for the recovery of rotors of large-scale hydraulic turbines. J. Mater. Process. Technol., 231–238.

Bremer, C., 2005. Automated repair and overhaul of aero-engine and industrial gas turbine components. In: Proceedings of the ASME Turbo Expo, Reno-Tahoe, Nevada, USA.

Bunker, R.S., 2009. The effects of manufacturing tolerances on gas turbine cooling. ASME J. Turbomach. 131 (4), 041018.

Dutta, B., Palaniswamy, S., Choi, J., Song, L.J., Mazumder, J., 2011. Additive manufacturing by direct metal deposition. Adv. Mater. Process. 169 (5), 33–36.

Eiamsa-ard, K., Nair, H.J., Ren, L., Ruan, J., Sparks, T., Liou, F., 2005. Part repair using a hybrid manufacturing system. In: Proceedings of the Sixteenth Annual Solid Freeform Fabrication Symposium, Austin, TX.

Franco, A., Lanzetta, M., Romoli, L., 2010. Experimental analysis of selective laser sintering of polyamide powders: an energy perspective. J. Clean. Prod. 18 (16), 1722–1730.

Francoeur, M., 2002. Laser Die Repair. October 2002. Industrial Laser Solutions. The Interantioanl Resource for Laser Materials Processing, PennWell Corporation, Tulsa, OK.

Frischknecht, R., Jungbluth, N., Althaus, H.-J., Doka, G., Dones, R., Hischier, R., Hellweg, S., Nemecek, T., Rebitzer, G., Spielmann, M., 2007. Final report ecoinvent data v2.0, No. 1. In: Overview and Methodology. Swiss Centre for Life Cycle Inventories, Dübendorf, CH.

Ganesh, P., Kaul, R., Paul, C.P., Tiwari, P., Rai, S.K., Prasad, R.C., Kukreja, L.M., 2010. Fatigue and fracture toughness characteristics of laser rapid manufactured Inconel 625 structures. Mater. Sci. Eng. A 527 (29–30), 7490–7497.

Gao, J., Yilmaz, O., Noble, D., Gindy, N., 2008. An integrated adaptive repair solution for complex aerospace components through geometry reconstruction. Int. J. Adv. Manuf. Technol. 36, 1170–1179.

Gao, J., Chen, X., Zheng, D., 2010. Remanufacturing oriented adaptive repair system for worn components. In: Proceedings of Responsive Manufacturing – Green Manufacturing ICRM, 5th International Conference, pp. 13–18 http://dx.doi.org/10.1049/cp.2010.0406. Ningbo, China.

Grant, G., Tabakoff, W., 1975. Erosion prediction in turbomachinery resulting from environmental particles. J. Aircr. 12 (5), 471–478.

Griffith, M.L., 2000. Understanding the microstructure and properties of components fabricated by laser engineered net shaping (LENS™). Mat. Res. Soc. Symp. Proc. 625. Warrendale, PA: MRS, 2000.

Gutowski, T., Sahni, S., Boustani, A., Graves, S., 2011. Remanufacturing and energy savings. Environ. Sci. Technol. 45, 4540–4547.

Hamed, A., Tabakoff, W., Wenglarz, R., 2006. Erosion and deposition in turbomachinery. J. Propul. Power 22, 350–360.

Hedges, M., Calder, N., 2006. Near net shape rapid manufacture & repair by LENS. In: Proceedings of Cost Effective Manufacture via Net-Shape Processing, Neuilly-sur-Seine, France, pp. 13–21-13-4.

LENS Technology, 2011. http://www.optomec.com/Additive-Manufacturing-Technology/Laser-Additive-Manufacturing (accessed 22.12.11.).

Margolis, N., Jamison, K., Dove, L., 1999. Energy and Environmental Profile of the U.S. Metal Casting Industry. U.S. Department of Energy, Office of Industrial Technologies, Washington, D.C.. http://energy.gov/sites/prod/files/2013/11/f4/profile_0.pdf

Michaud, C., Llerena, D., 2006. An economic perspective on remanufactured products: industrial and consumption challenges for life cycle engineering. In: Proceedings of 13th Cirp International Conference On Life Cycle Engineering, Heverlee, Belgium.

Mohaghegh, K., Sadeghi, M.H., Abdullah, A., Boutorabi, R., 2010. Improvement of reverse-engineered turbine blades using construction geometry. Int. J. Adv. Manuf. Tech. 49 (5–8), 675–687.

Morrow, W.R., Qi, H., Kim, I., Mazumder, J., Skerlos, S.J., 2007. Environmental aspects of laser-based and conventional tool and die manufacturing. J. Clean. Prod. 15 (10), 932–943.

Östlin, J., Sundin, E., Björkman, M., 2009. Product life-cycle implications for remanufacturing strategies. J. Clean. Prod. 17 (11), 999–1009,.

Paul, C.P., Ganesh, P., Mishra, S.K., Bhargava, P., Negi, J., Nath, A.K., 2007. Investigating laser rapid manufacturing for Inconel-625 components. Opt. Laser Technol. 39 (4), 800–805.

Pinkerton, A.J., Wang, W., Li, L., 2008. Component repair using laser direct metal deposition. Proc. IMechE Part B J. Eng. Manuf. 222 (7), 827–836.

Piya, C., Wilson, J.M., Murugappan, S., Shin, Y., Ramani, K., 2011. Virtual repair: geometric reconstruction for remanufacturing gas turbine blades. In: Proceedings of the ASME 2011 International Design Engineering Technical Conferences & Design for Manufacturing and the Life Cycle Conference, Washington D.C., USA. 2011.

Ramani, K., Ramanujan, D., Bernstein, W.Z., Zhao, F., Sutherland, J.W., Handwerker, Choi C.J., Kim, K.H., Thurston, D., 2010. Integrated sustainable life cycle design: a review. J. Mech. Des. 132, 9.

Roy, S., Francoeur, M., 2002. Options for Restoring Molds. Sept. 1. Joining Technologies, Cincinnati, OH. http://www.moldmakingtechnology.com/articles/options-for-restoring-molds.

Santos, E.C., Shiomi, M., Osakada, K., Laoui, T., 2006. Rapid manufacturing of metal components by laser forming. Int. J. Mach. Tools Manuf. 46, 1459–1468.

Sellamani, S., Muthuganapathy, R., Kalyanaraman, Y., Murugappan, S., Goyal, M., Ramani, K., Hoffman, C.M., 2010. PCS: prominent cross-sections for mesh models. Comput. Aided Des. Appl. 7, 601–620.

Smith, V.M., Keoleian, G.A., 2004. The value of remanufactured engines: life-cycle environmental and economic perspectives. J. Ind. Ecol. 8 (1–2), 193–221 http://dx.doi.org/10.1162/1088198041269463.

Sutherland, J.W., Skerlos, S.J., Olson, W.W., Gunter, K.L., Khadke, K., Zimmerman, J., 2003. Environmentally benign manufacturing: status and vision for the future. In: Proceedings of NAMRI/SME Transactions, Dearborn, MI.

US Environmental Protection Agency (EPA), 2009. Toxics Release Inventory (TRI) 2007. Report available at: http://www.epa.gov/tri/tridata/tri07/index.htm.

Xue, L., Islam, M., 2002. Laser consolidation – a novel one-step manufacturing process from CAD models to net- shape functional components. In: Keicher, D., Sears, J., Smugeresky, J. (Eds.), International Conference on Metal Powder Deposition for Rapid Manufacturing, MPIF, Providence, RI.

Yilmaz, O., Gindy, N., Gao, J., 2010. A repair and overhaul methodology for aero-engine components. Robot. Comput Integr. Manuf. 26 (2), 190–201.

Yilmaz, O., Noble, D., Gao, J., 2005. A study of turbomachinery components machining and repairing methodologies. Aircr. Eng. Aerosp. Technol. Int. J. 77 (6), 455–466.

Zhang, Y.M., Li, P., Chen, Y., Male, A.T., 2002. Automated system for welding-based rapid prototyping. Mechatronics 12 (1), 37–53.